
SUPERNOVA REMNANT SNR 1987A IN THE MID-INFRARED AT 18 YEARS

Patrice Bouchet (1) — Eli Dwek (2) — John Danziger (3) — Richard G. Arendt (4) — I. James M. De Buizer (5)

(1) GEPI, Observatoire de Paris, and Cerro Tololo Inter-American Observatory (CTIO); (2) NASA Goddard Space Flight Center, USA; (3) Osservatorio Astronomico di Trieste, Italy; (4) Science Systems & Applications, Inc. (SSAI), NASA Goddard Space Flight Center, USA; (5) Gemini Observatory, Chile

ABSTRACT. We present high resolution 11.7 and 18.3 μm images of SN 1987A obtained on day 6526 with the Gemini South 8m telescope. Nearly contemporaneous spectra obtained with Spitzer show that the emission consists of thermal emission from silicate dust. We show that either the dust is collisionally heated by the X-ray emitting plasma, or it could be radiatively heated in the dense UV-optical knots that are overrun by the advancing supernova blast wave. In either case the dust-to-gas mass ratio in the circumstellar medium around the supernova is significantly lower than that in the general interstellar medium of the LMC, suggesting either a low condensation efficiency, or the efficient destruction of the dust by the SN blast wave. This work clearly illustrates also the need to complement mid-infrared spectroscopic observations carried out from space with imaging at relatively high angular resolution from ground based instruments.

RÉSUMÉ. Nous présentons des images de SN 1987A obtenues au jour 6526 à 11.7 et 18.3 μm avec le télescope de 8-m de Gemini. Des spectres obtenus presque simultanément avec Spitzer montrent que cette émission est une émission thermique de poussières de silicates. Nous montrons que les poussières pourraient être réchauffées soit par collision dans le plasma émetteur en rayons X, soit par radiation à l'intérieur des noeuds denses observés dans l'UV et le visible, qui sont emboutis par l'onde de choc créée par la supernova. Dans les deux cas, la valeur du rapport poussières à gaz dans le milieu circumstellaire de la supernova est clairement inférieure à celle du milieu interstellaire du PNM, ce qui suggère, soit que leur condensation a été inefficace, soit que les mécanismes de destruction par le soufflement de l'onde de choc sont au contraire très efficaces. Ce travail montre l'importance de compléter des observations obtenues depuis l'espace par d'autres obtenues avec une meilleure résolution spatiale depuis le sol.

KEYWORDS: Stars: Supernovae: Individual: SN 1987A — Infrared: ISM: Dust, Supernova Remnants

MOTS-CLÉS: Étoiles : Supernovae : Individuelle : SN 1987A — Infrarouge : ISM : Poussières, Restes de supernovae

1. Based on observations obtained at the *Gemini* Observatory, which is operated by the Association of Universities for Research in Astronomy (AURA), Inc. under cooperative agreement with the NSF on behalf of the *Gemini* partnership. CTIO is a division of the National Optical Astronomy Observatory (NOAO) operated by the Association of Universities for Research in Astronomy (AURA), Inc. under cooperative agreement with the National Science Foundation.

1. INTRODUCTION

The collision between the ejecta of SN 1987A and the circumstellar inner equatorial ring (ER) is now underway. At UV-optical (UVO) wavelengths, “hot spots” have appeared inside the ER (Pun et al., 1997), and their brightness varies on time scales of a few months (Lawrence et al., 2000). There exist very few mid-infrared (IR) observations of supernovae in general. Therefore SN 1987A, the closest known supernova in 400 years, gives us an opportunity to explore the mid-IR properties of supernovae and the dust in their ejecta and surrounding medium with the help of the newest generation of large-aperture telescopes and sensitive mid-IR instrumentation like T-ReCS on the *Gemini*, in combination with IR data obtained from *Spitzer* Space Telescope (Werner et al. 2004). The first detection and analysis of mid-IR emission at the position of the supernova has been reported in Bouchet et al (2004), hereafter Paper I. Our last results are presented and discussed in depth in Bouchet et al. (2006), hereafter Paper II. We outline in this poster the main conclusions of this analysis.

2. OBSERVATIONS

Observations were carried out with T-ReCS attached at the *Gemini* South telescope in January 6, 2005 (day 6526) in the narrow Si5 filter ($\lambda_{eff} = 11.66 \mu\text{m}$; $\lambda = 11.09\text{-}12.22 \mu\text{m}$), and in February 1, 2005 (day 6552) in the Qa filter ($\lambda_{eff} = 18.30 \mu\text{m}$; $\lambda = 17.57\text{-}19.08 \mu\text{m}$). Results are presented in Figure 1. These images show several luminous “hot” spots distributed over the ring. The calibrated flux density integrated within an aperture of 1.3 arcsec radius is $F_\nu(11.7 \mu\text{m}) = 18.4 \pm 1.2 \text{ mJy}$ in the Si5 filter, and $F_\nu(18.3 \mu\text{m}) = 53.4 \pm 9 \text{ mJy}$ in the Qa filter.

A detailed discussion on the relation between the images obtained at various wavelengths can be found in Paper II. There is good overall agreement in shape and size between our IR image and images obtained from the X-ray to the radio. The most likely source for mid-IR radiation is thermal emission from warm dust. The X-ray radiation is thermal emission from very hot gas, whereas the optical emission arises from the dense knots in the ER that are overrun by slower shocks. The radio emission is likely to be synchrotron radiation from shock-accelerated electrons spiralling in the remnant’s magnetic field as stated by Dunne et al. (2003) and Manchester et al. (2005).

Observations were performed at the *Spitzer* Space Telescope on day 6184 with MIPS at $24 \mu\text{m}$, on day 6130 with IRAC in $3.6\text{-}8 \mu\text{m}$ region, and on day 6190 with IRS in the $12\text{-}37 \mu\text{m}$ (in its short (wavelength) – low (resolution), short-high, and long-high modes) (Houck et al., 2004).

3. DATA ANALYSIS

3.1. Spectral Analysis

The T-ReCS observations alone cannot discriminate between the different dust compositions. The comparison with the *Spitzer* observations clearly demonstrates that the IRS observations can be well fit with a silicate dust composition, ruling out graphite or carbon dust as major dust constituents in the circumstellar medium (see Figure 3). Line fluxes, centers and widths of the few signatures seen in the spectrum are given in Paper II. In our model the silicate temperature is $T_d = 180_{-15}^{+20} \text{ K}$, and the dust mass is $M_d = (1.1_{-0.5}^{+0.8}) \times 10^{-6} M_\odot$. We used the 11.7 and $18.3 \mu\text{m}$ T-ReCS images of the remnant to construct

black body temperature, and dust opacity maps of the ER (see Figure 1). The average dust temperature in these maps is $T_d = 166_{-12}^{+18}$ K. The average $11.7 \mu\text{m}$ optical depth per pixel is $\tau_d = (5.5_{-2.7}^{+4.2}) \times 10^{-6}$, and the total dust luminosity is $L_d = (2.3_{-0.4}^{+0.5}) \times 10^{36}$ erg s $^{-1}$, giving a dust mass $M_d = (2.6_{-1.4}^{+2.0}) \times 10^{-6} M_\odot$, in good agreement with the total mass obtained from the spectral analysis of the ER.

3.2. The Origin of the Mid-Infrared Emission

Our data show unambiguously that the emission is thermal emission from dust. At issue are the location and heating mechanism of the dust. The forward expanding non-radiative blast wave is currently interacting with the circumstellar material and the knots in the ER. The interaction of the blast wave with the knots transmits lower velocity radiative shocks into these dense regions, producing soft X-rays and the “hot spots” seen in the *HST* images. The interaction of the blast wave with the dense knots also generates reflected shocks that propagate back into the medium that was previously shocked by the expanding SN blast wave. The complex morphology and density structure of the ER gives rise to a multitude of shocks characterized by different velocity, temperatures, and post shock densities.

The mid-IR images cannot determine the location of the radiating dust, whether it resides in the X-ray emitting gas or in the denser UVO emitting knots. Therefore, we cannot, a priori, assume a particular dust heating mechanism: collisional heating in the shocked gas, or radiative heating in the radiative shocks.

3.3. Dust in the X-ray Emitting Gas

The morphological similarities between the $11.7 \mu\text{m}$ emission, dust temperature, and optical depth maps on one hand and the X-ray maps of the supernova on the other hand suggests that the dust giving rise to the IR emission may be well mixed with the X-ray emitting gas. We argue in Paper II that for average conditions in the X-ray plasma the dust heating in the X-ray gas is dominated by electronic collisions.

3.3.1. The Dust Temperature

X-ray observations show the presence of two X-ray emission components (Park et al., 2005): one associated with the “slow shock” with an electron temperature of ~ 0.23 keV and a density of $n_e \sim 6000 \text{ cm}^{-3}$, and the second, associated with the “fast shock” with electron temperatures and densities of $kT \sim 2.2$ keV and $n_e \sim 280 \text{ cm}^{-3}$, respectively. The latestest *Chandra* data indicate (Park et al., 2006) that the “fast shock” and the “slow shock” of the model are becoming less distinguishable. Albeit rather speculative, the overall temperature might thus be “merging” onto an “average” temperature of $kT \sim 1.5$ keV $\sim 1.8 \times 10^7$ K, and intermediate electron densities. We show that the range of densities expected for this “average” shock is in very good agreement with that implied from the IR observations.

3.3.2. The Infrared-to-X-ray Flux Ratio (IRX)

For a given dust-to-gas mass ratio and grain size distribution, an important diagnostic of a dusty plasma is the infrared-to-X-ray flux ratio *IRX*, defined as the infrared cooling to X-ray cooling in the 0.2–4.0 keV band (Dwek, 1987). From the January 2005 *Chandra* data, we estimate the X-ray flux in the 0.2–4.0 keV X-ray band to be 7.24×10^{-12} erg cm $^{-2}$ s $^{-1}$ after correcting for interstellar absorption by an H-column density of $N_H = 2.35 \times 10^{21}$ cm $^{-2}$. The total IR flux is $F_{IR} = 7.7 \times 10^{-12}$ erg cm $^{-2}$ s $^{-1}$ which leads to an *IRX* ratio ~ 1 . This value is much lower than the theoretical value of $\sim 10^2$, expected for a

$T_e \approx 1.8 \times 10^7$ K plasma, which is observed in the young remnants Tycho and Cas A. Other (mostly older) SNRs with measurable IR emission show somewhat lower IRX ratios, but not as low as SNR 1987A (Dwek et al., 1987). Several effects could be the cause for this very low value of the IRX ratio in SNR 1987A.

First, in remnants the IRX ratio was calculated by Dwek (1987) for an interstellar dust-to-gas mass ratio of 0.0075. The SNR 1987A blast wave is expanding into the circumstellar shell of its progenitor star, which, a priori, is not expected to have an interstellar dust-to-gas mass ratio. Moreover, when estimating the depletion of elements onto dust in the ER, we should compare the expected dust abundances in the ER with the maximum available abundances for the LMC. We show in Paper II, however, that under plausible assumptions, the IRX ratio in the ER should be about 0.5–0.7 times that expected from Supernova Remnants in the Milky Way, still significantly larger than implied from the observations. The extremely low value of the IRX ratio may therefore be due to a deficiency in the abundance of the dust, compared to interstellar values, which may reflect the low condensation efficiency of the dust in the circumstellar envelope.

Second, the dust deficiency could be the result of grain destruction by thermal sputtering in the hot gas. According to Dwek et al. (1996) the sputtering lifetime, τ_{sput} , in a plasma with temperatures above $\sim 10^6$ K is:

$$\tau_{sput} \approx 3 \times 10^5 \frac{a(\mu\text{m})}{n(\text{cm}^{-3})} \text{ yr} \quad [1]$$

where n is the density of nucleons in the gas. The X-ray emitting gas is highly ionized, and we assume that its density is that required to heat the dust to the observed range of temperatures, that is, $n \approx 300$ to 1400 cm^{-3} . Grain destruction is important when the sputtering lifetime is about equal to the age of the shocked gas, which we take to be ~ 1 yr. The low IRX ratio can therefore be attributed to the effects of grain destruction if the dust particles had initial radii between 10 and 50 Å. So attributing the small IRX ratio to the effect of grain destruction in the hot plasma requires that only small grains had formed in the presupernova phase of the evolution of the progenitor star. The low IRX ratio shows that IR emission from collisionally heated dust is not the dominant coolant of the shocked gas. Its lower than expected value suggests a dust-to-gas mass ratio in the ER that is only a few percent of its interstellar value. The puzzle of the low dust abundance is greater if, in fact, the IR emission arises from dust that is *not* embedded in the X-ray emitting gas, but from dust that resides in the UV/optical knots instead.

3.4. Dust in the Dense Knots of the Equatorial Ring

The UVO light emitting knots discovered with the *HST* resemble a string of beads uniformly distributed along the ER. Figure 3 depicts the map of the dust optical depth overlaid with the *HST* emission obtained on Dec 15, 2004 (day 6502), the closest to our $11.7 \mu\text{m}$ observations. The data look very similar, but the IR emission seems to emanate from a somewhat wider region than the optical emission, an effect that cannot be entirely accounted for by the lower resolution of the IR data as shown in Figure 2.

Nevertheless the good correlation between the IR emission maps and the *HST* image, suggest that a significant fraction, if not most, of the mid-IR emission may be emanating from the knots. In Paper II we compute the energy density in the knot studied by Pun et al. (2002), and we show that the average dust temperature should be ~ 125 K, in reasonable agreement with the observed average. The total mass of radiating dust is found to be $\sim 10^{-6} M_\odot$. The typical mass of gas in a knot of radius $r = 2 \times 10^{16}$ cm, and density $n_0 = 10^4 \text{ cm}^{-3}$ is $\sim 10^{-4} M_\odot$. If $\mathcal{N} \approx 20$ is the number of knots in the ER, then the dust-to-gas mass ratio is $\sim 10^{-6}/(\mathcal{N} \times 10^{-4}) \approx 5 \times 10^{-4}$, or approximately a factor of 10 less than the average dust-to-gas mass ratio in the local interstellar medium.

The low abundance of dust in the knots could be explained if the dust is efficiently destroyed in the shocked gas *and* if the transmitted shocks have already traversed most of the volume of the knots. Calculations presented by Jones (2004) show that about 49% of the silicate grains swept up by 200 km s^{-1} shocks expanding into a medium with a preshocked density of 0.25 cm^{-3} are destroyed. This fraction could be significantly higher for the densities encountered by the shocks traversing the knots. This scenario predicts that the IR emission from the knots was higher in the past, contrary to observed IR light curves (see Paper II). Therefore, if the IR emission emanates from the knots, the low dust abundance must reflect the initial dust abundance in these objects.

4. CONCLUSIONS

In order to assess the role of SNe in the production of dust in the Universe, it is clearly important to measure the presence of dust that survives into the formation of the remnant, and for this, mid-IR and sub-mm observations are critical. Our high angular imaging ground based mid-IR observations needed to be complemented with spectroscopic data from *Spitzer*, and a multiwavelength analysis was essential for reaching our conclusions.

Acknowledgements

We thank the SAINTS collaboration (PI: R. Kirshner) for kindly providing us with the last *HST* data, D. Manchester for providing us with the *ATCA* data, and S. Park for providing us with the *Chandra* data and for fruitful discussions.

5. References

- Bouchet, P., et al., 2004, *Astrophys. J.* , 611, 394 (Paper I)
 Bouchet, P., et al., 2006, *ApJ*. in press; astro-ph:0601495 (Paper II)
 Dunne, L., et al., 2003, *Nature* , 424, 285
 Dwek, E., 1987, *Astrophys. J.* , 322, 812
 Dwek, E., et al., 1987, *Astrophys. J.* , 320, L27
 Dwek, E., Foster, S. M., & Vancura, O. 1996, *Astrophys. J.* , 457, 244
 Houck, J., et al., *Astrophys. J. Suppl.* , 154, 18
 Jones, A.P., 2004, in *Astrophysics of Dust*, ASP Conf. Series vol 309, eds. A.N. Witt, et al. (ASP - San Francisco), p.347
 Lawrence, S.S., et al., 2000, *Astrophys. J.* , 537,123
 Manchester, D., et al., 2005, *Astrophys. J.* , 628, 131
 Park, S., et al., 2005, *Astrophys. J.* , 634, L73
 Park, S., et al., 2006, *Astrophys. J.* , 646, 1001
 Pun, C.S.J., et al., 1997, *IAU Circ.* , 6665, 1
 Pun, C.S.J., et al., 2002, *Astrophys. J.* , 572, 906
 Werner, M., et al., 2004, 154, 1

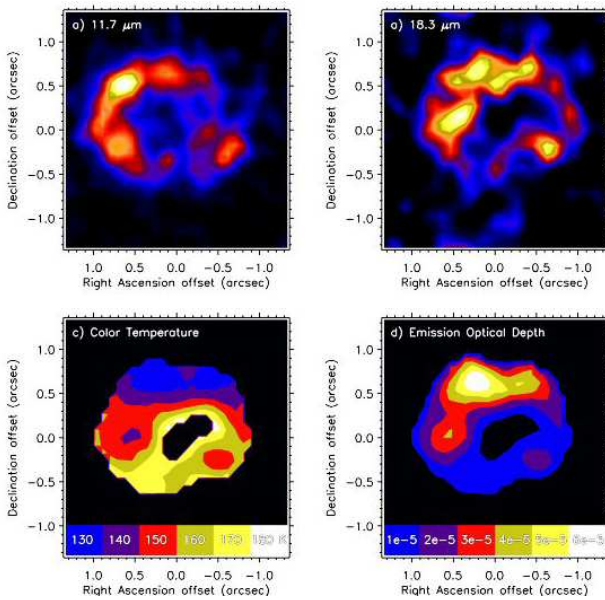


Figure 1. (a) SN 1987A seen with T-ReCS at day 6526 in the Si5 narrow band filter (11.7 μm) and (b) at day 6552 in the Qa filter (18.3 μm); (c) temperature map assuming pure black body emission; (d) Opacity map resulting from the same algorithm. These images are smoothed 2 pixels (0.18 arcsec).

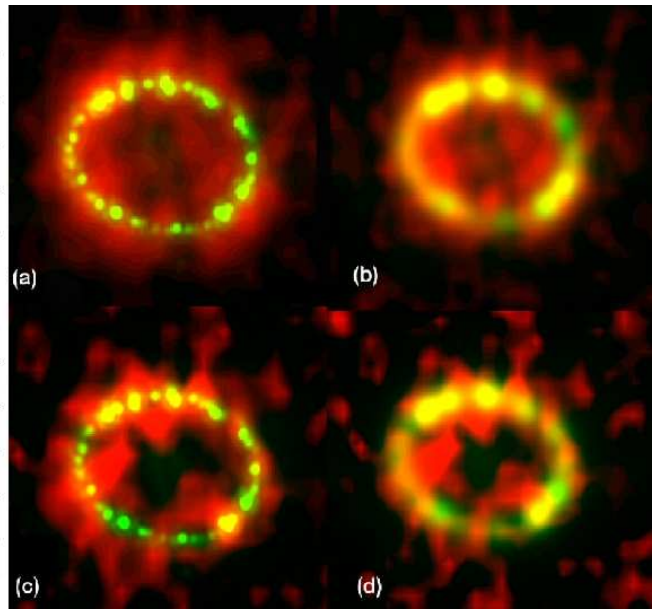


Figure 2. (a) Montage of the mid-IR 11.7 μm image of the ER (red) and the HST F625W image obtained on day 6502 (yellow); (b) same as (a) with the HST image (yellow) convolved to match the resolution of the T-ReCS 11.7 μm image (red); (c) montage of the Qa image from T-ReCS (red) with the HST F625W image (yellow); (d) same as (c) with the HST image convolved to match the T-ReCS Qa angular resolution.

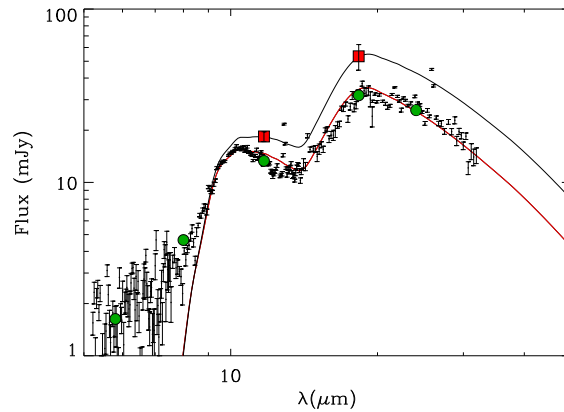


Figure 3. The Spitzer IRS spectrum fitted with a silicate dust model. Green circles: Spitzer flux measurements. This model has been scaled to fit the T-ReCS flux measurements (red squares). Note that the mid-IR emission has been brightening significantly between both sets of observations. The Spitzer IRS data unambiguously show that silicate are the major dust component. The derived parameters of the fit are: $T = 180^{+30}_{-20}$ K, $M_{dust} = 0.7 - 1.7 \times 10^{-6} M_{\odot}$, and $L_{IR} = 1.6 \pm 0.3 \times 10^{36}$ erg s $^{-1}$.